

Quantitative *in situ* TEM tensile testing of an individual nickel nanowire

Yang Lu¹, Cheng Peng¹, Yogeewaran Ganesan¹, Jian Yu Huang²
and Jun Lou¹

¹ Department of Mechanical Engineering and Materials Science, Rice University, Houston, TX 77005, USA

² Center for Integration Nanotechnologies (CINT), Sandia National Laboratories, Albuquerque, NM 87185, USA

E-mail: jlou@rice.edu

Received 17 May 2011, in final form 4 July 2011

Published 5 August 2011

Online at stacks.iop.org/Nano/22/355702

Abstract

In this paper, we have demonstrated the usage of a novel micro-mechanical device (MMD) to perform quantitative *in situ* tensile tests on individual metallic nanowires inside a transmission electron microscope (TEM). Our preliminary experiment on a 360 nm diameter nickel nanowire showed that the sample fractured at an engineering stress of ~ 1.2 GPa and an engineering strain of $\sim 4\%$, which is consistent with earlier experiments performed inside a scanning electron microscope (SEM). With *in situ* high resolution TEM imaging and diffraction capabilities, this novel experimental set-up could provide unique opportunities to reveal the underlying deformation and damage mechanisms for metals at the nanoscale.

 Online supplementary data available from stacks.iop.org/Nano/22/355702/mmedia

(Some figures in this article are in colour only in the electronic version)

1. Introduction

Deformation mechanisms of metallic nanostructures, such as nanowires and nanopillars, have drawn considerable interest in the past decade due to their importance in building reliable nanoelectronic devices and predicting the performance of nano-electromechanical systems (NEMS) [1–5]. Recently, *in situ* TEM mechanical testing has emerged as a powerful tool to interrogate low-dimensional metallic nanostructures, since it could provide detailed structural information at very high resolution during mechanical testing of such samples. This unique capability of monitoring a sample's internal structural evolution in real time is considered to be very valuable in establishing a better correlated structure–property relationship. Various *in situ* TEM mechanical testing methods have been developed in the past decade, such as nanoindentation tests of metal thin films [6], nanocompression tests of metal pillars [7–10] and bending/buckling tests [11–13] or resonances/vibration-based tests of nanowires [14, 15]. However, reliable and easy-to-interpret tensile tests remain to be rather challenging, owing to the difficulties associated with sample clamping,

precise manipulation and alignment, as well as accurate measurement of load and displacement. Earlier efforts that had been made on developing *in situ* TEM tensile testing of low-dimensional nanomaterials, such as AFM cantilever or nanomanipulator assisted methods [16–19], often encounter inevitable drawbacks such as uncontrollable sample geometry and limited material selectivity, and problematic sample alignment and clamping. In order to develop a robust universal testing platform for samples of different materials and sizes/geometries, micro-electromechanical system (MEMS) has been considered as an ideal solution to perform nanoscale mechanical testing for various types of samples. Carbon nanotubes [20–22], bio-fibrils [23, 24], thin films [25] and nanowires [20, 26] have already been successfully tested by different MEMS devices. Also, due to their small footprints, MEMS-based testing devices can naturally fit into SEM/TEM chambers for *in situ* mechanical testing [27]. We have recently designed and fabricated a silicon-based micro-mechanical device (MMD) to perform quantitative *in situ* tensile tests on 1D nanomaterials within a scanning electron microscope equipped with a quantitative nanoindenter [28, 29]. This device was actuated mechanically with direct and independent

measurement of load and displacement at high precision, allowing real-time observation of the deforming samples. Various samples, such as MWCNTs, Ni, Cu and Au NWs, had been tested using the MMD platforms assisted by a quantitative nanoindenter inside an SEM [28–30]. This platform has demonstrated its strength in providing continuous high resolution force–displacement data, and versatile and precise load/displacement control, due to the simplified device structure and independent actuation and sensing mechanisms.

On the other hand, metallic nanowires (including Ni NWs) have stimulated great interest recently as important building blocks for future nanoscale electronic and electromechanical devices in various applications. Due to its unique magnetic properties, nickel nanowires can be precisely manipulated by a controlled external magnetic field [31]. Furthermore, once functionalized, nickel nanowires also have a potential for drug delivery and intracellular sensing. For instance, by using their different surface binding effects for specific chemical or biological targets, researchers combined nickel and gold segments into single 1D metallic nanostructures (Au/Ni bimetal nanowires) to achieve remarkable new features that can be used in novel biomedical applications, such as controllable gene delivery [32]. However, the ability to achieve the full potentials of these fascinating technologies is ultimately limited by how these one-dimensional building blocks will behave at relevant length scales, in particular their mechanical performance and reliability.

In the current work, we have successfully extended the usage of the novel micro-mechanical device to perform quantitative *in situ* TEM tensile test on an individual nickel nanowire. Aided by a high resolution Nanofactory™ TEM-nanoindenter holder (figure 1(a)), individual nickel nanowires with diameters around 300 nm were tested *in situ* and sample stress versus strain data were simultaneously obtained. The real-time TEM images and diffraction analysis provided very useful insights into the origin of high strength and corresponding fracture mechanism.

2. Device description and sample preparation

The design and fabrication of the micro-mechanical device (MMD) had been described in detail elsewhere [28, 29] and will only be briefly discussed here. The MMD (figure 1(b)) was fabricated on SOI (silicon-on-insulator) wafers using standard photolithography techniques. The device can convert the compression applied by a quantitative nanoindenter into uniaxial tension on samples clamped between the suspended sample stages through a simple ‘push–pull’ mechanism (figures 1(b)–(d)). The force versus displacement and thus stress versus strain curves (in conjunction with real-time sample dimension measurements) of the sample could be derived from the force and displacement reading of the nanoindenter, with the help of finite element analysis (FEA) [28] or a simple response subtraction method [29].

It should be noted that, while the MMD was originally designed with the consideration of its usage in a transmission electron microscope (TEM) in mind [29], we still needed to modify the design layout considerably in order for it to work

properly with the Nanofactory™ *in situ* TEM-nanoindenter sample holder. The new design (as shown in figures 1(a) and (b)) modifications include further decreasing the device size (device footprint decreased from 3 mm × 2 mm to 2.5 mm × 1.2 mm) for better fitting into the highly restricted sample space in the holder (figure 1(a)); decreasing the device weight by reducing the thickness of the suspended Si device layer (reduced from the original $9.5 \pm 0.5 \mu\text{m}$ to the current $6 \pm 0.5 \mu\text{m}$ thickness) to improve the stability of the device when it is being coarsely aligned by using the piezo-driven positioning stage in the holder or being set in motion during the actual testing; and finally revising the back-side window design to facilitate in TEM-nanoindenter tip positioning while maintaining proper electron beam alignment. Figure 1(a) shows an optical image of a Nanofactory™ TEM-Nanoindenter sample holder loaded with a newly designed MMD.

Nickel nanowire samples tested in this study were fabricated by a simple aluminum anodic oxide (AAO) template-assisted electrochemical deposition process [29, 31]. Careful TEM diffraction analysis at multiple locations along the nanowire axial direction was performed, confirming these Ni nanowires possess single-crystalline face centered cubic (fcc) structure with [112] orientation along the wire axis [31]. Once the nanowires were released from the AAO template, a micromanipulator under an optical microscope or a nanomanipulator inside an SEM was used, depending on sample dimensions [29], to pick up an individual nanowire and place it between the sample stages. Sample clamping was realized by using either a conductive epoxy or an FIB-deposited metal layer [29, 30]. As shown in figure 1(d), a ~ 300 nm Ni nanowire was placed and clamped between two sample stages using conductive epoxy.

Once loaded with a nanowire sample, the MMD was then attached to a gold or tungsten rod with conductive silver glue to create an electrical conductive path in order to minimize charging issues. The rod with the MMD was then fixed on a copper cap which was subsequently attached to the ball head driven by a piezo-tube (left part in figure 1(a)). This set-up makes it possible for device motion in three-dimensional spaces with respect to the nanoindenter head on the right side in figure 1(a). The quantitative nanoindenter is equipped with a blunted diamond tip connected to a simple cantilever-beam-based force sensor [33], which requires careful on-site calibration before the actual experiment takes place. All experiments were performed inside an FEI™ Tecnai G² F30 high resolution TEM, operated at 300 kV working voltage.

3. Results and discussions

Figure 2 demonstrated a successful *in situ* TEM testing of a ~ 360 nm nickel nanowire. The sample gauge length defined by the distance between two clamping point of the nanowire sample was determined to be $\sim 15 \mu\text{m}$, using high resolution SEM images before transporting the sample-loaded device into the TEM.

Displacement control was used in the actual test. The automatic quantitative nanoindentation test executed by the

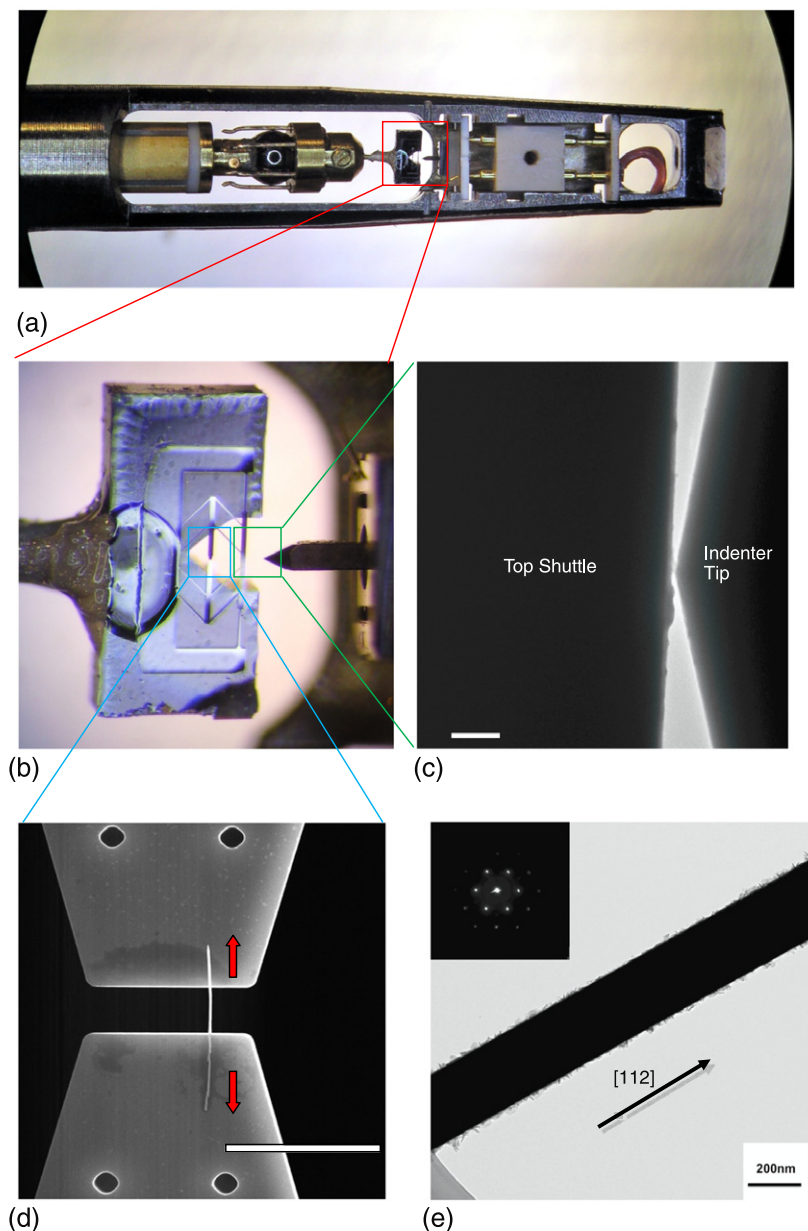


Figure 1. *In situ* TEM tensile testing set-up: (a) a micro-mechanical device (MMD) loaded in the Nanofactory™ TEM-nanoindenter sample holder; (b) close-up view of the nanoindenter head toward the MMD; (c) a TEM image showing the alignment of the nanoindenter head with the center position of the top shuttle beam of the MMD (scale bar 1 μm); (d) an SEM image showing a ~ 300 nm nickel nanowire clamped between two sample shuttles (scale bar 20 μm); and (e) a TEM image of an undeformed nickel nanowire with corresponding selected-area diffraction (SAD) pattern (scale bar 200 nm).

automatic function in the control software has a relatively small displacement range of ± 770 nm. However, for this specific ~ 360 nm diameter Ni NW, a preliminary automatic test indicated that the sample remained in an elastic region after reaching the full ± 770 nm indentation displacement limit. In order to perform a complete tensile test up to fracture, we have to first perform a manual indentation by using the coarse movement function, which has tens to hundreds of microns in displacement range and was typically utilized for sample/device manipulation and alignment. During this coarse movement, applied force can still be recorded by the nanoindenter force sensor, while the sample displacement can

be monitored through the real-time TEM videos. By carefully performing manual indentation on the sample under larger elastic deformation, an automatic indentation experiment was then engaged and continuously stretched the nanowire sample until the sample comes into plastic deformation and final fracture. Figure 2(b) showed the sample right before fracture, which was under significant plastic deformation (as indicated by the red double arrows). Finally the sample suddenly broke without an observable necking process (figure 2(c)).

Post data analysis was executed to convert the original nanoindenter force versus displacement reading from the testing into a sample stress versus strain curve. This conversion

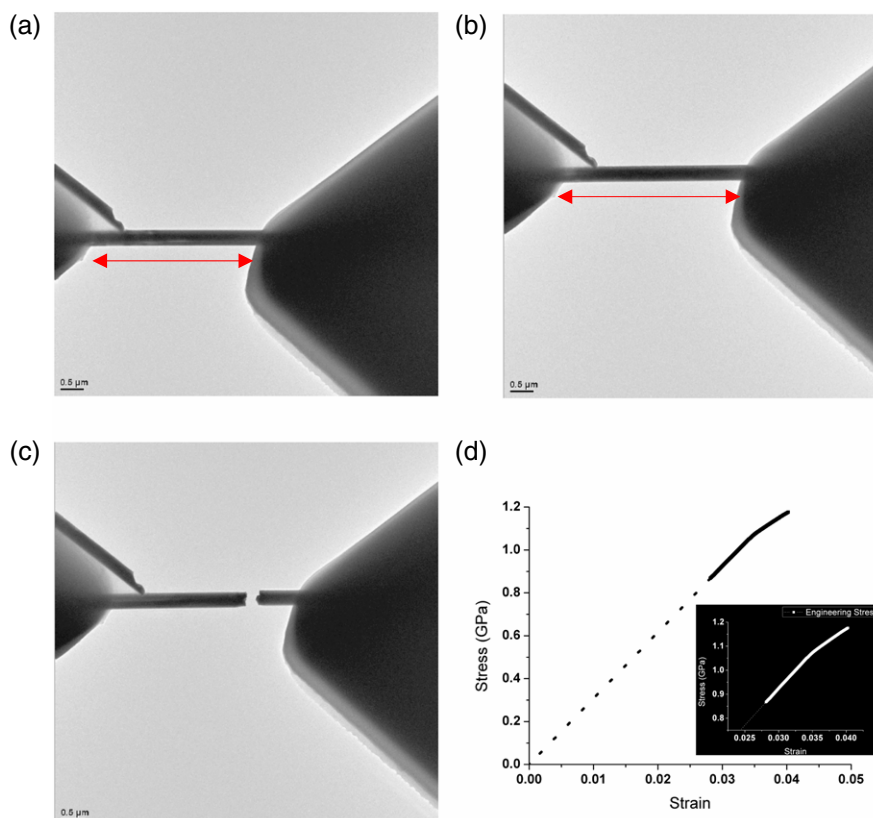


Figure 2. TEM image frames showing a quantitative tensile test for a ~ 360 nm diameter nickel nanowire (scale bars $0.5 \mu\text{m}$): (a) before loading; (b) right before breaking; (c) after breaking; and (d) the corresponding sample stress versus strain curves, while the dashed line corresponds to the coarse manual loading region (the inset shows a magnified view of the automatic loading region with high resolution data acquisition).

relationship was obtained by fitting and comparing the slopes of an empty device and the initial linear region of the actual test, and the details can be found in [29]. By converting the indenter force–displacement data into sample force and displacement data, together with the geometry (diameter, elongation of the nanowire) information from the video, the stress versus strain curve can be obtained (figure 2(d)). It might be noted that, due to the limited range (± 770 nm) of the automatic indentation function, manual loading was employed prior to the engagement of the automatic loading in order to break the sample. The inset in figure 2(d) shows the stress versus strain data during the automatic testing stage.

In figure 2(d), the specific nanowire sample experienced a total $\sim 4\%$ strain before final fracture. Typical plastic flow behavior was not observed from the stress–strain curve, but the sample did show a slope change (slightly lower) at about 1.1 GPa, which may indicate the onset of the local plastic deformation activities. However, the incipient plasticity in this sample might occur at a much lower strain level, that is possibly below the detection limit of the current technique. The sample breaking strength is about 1.2 GPa, which is much higher than bulk Ni (140–195 MPa, [34]). According to the earlier work done on similar Ni NW samples [29], the measurement using this set-up appears quite consistent with the results from earlier *in situ* SEM measurements.

Finally, from the supplementary movie (available at stacks.iop.org/Nano/22/355702/mmedia) (corresponding to the test

in figure 2), dramatic contrast changes within the strained nanowire sample imaged under bright-field TEM imaging conditions were clearly observed (Figures 2(a)–(c)), until the sample eventually broke at the position within the sample region that underwent the significant contrast changes. Similar phenomena had been reported, such as the *in situ* testing of ZnO nanowires by Espinosa *et al* [35] in which several fringes was evident in the bright-field TEM image and the sample did break along one of such fringes. It was believed that the local changes observed in the contrast of the TEM images might be related to atomic distortions resulting from stress concentrations [35]. In order to verify this assumption, and reveal the underlying deformation mechanism, high magnification TEM imaging can be performed during the test. For example, with appropriate orientation, dislocation networks and their interactions with excellent contrast may be observed in real-time bright-field TEM images (figure 3(a)). For the Ni NW tested in figure 2, higher magnification image showed very clear fracture morphology (figure 3(b)), which convincingly verified the earlier suggestion of brittle fracture based only on a stress–strain curve and low magnification video of the deformation and fracture processes. This also agreed well with the results of earlier SEM experiments [29]. Additionally, selected-area diffraction (SAD) analysis, a unique and important capability of TEM, could also offer very useful insights into crystalline structure evolution such as the possible phase transformation [36, 37] during the mechanical

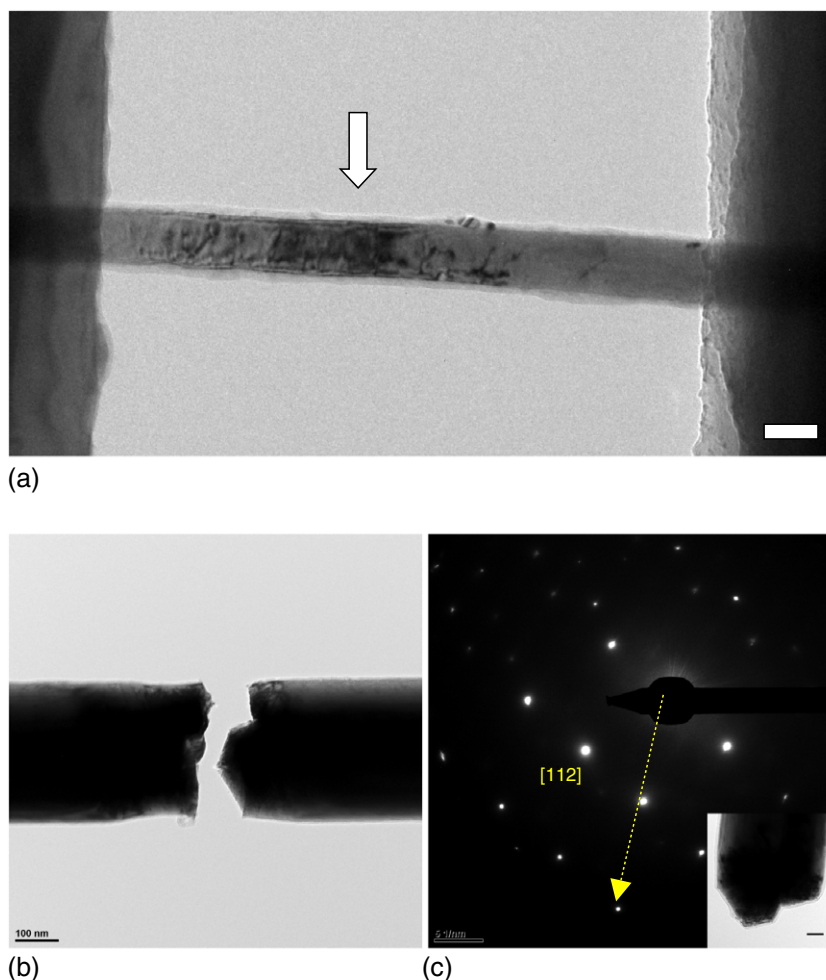


Figure 3. High magnification TEM image and diffraction analysis: (a) a ~ 300 nm nickel nanowire under tension, the image contrast of the middle section (indicated by the white arrow) showing dislocation networks (scale bar 200 nm); (b) close-up view of the fracture morphology of the sample fractured in the test of figure 2 (scale bar 100 nm); and (c) real-time TEM selected-area diffraction (SAD) analysis showing the crystalline structure of the broken nanowire sample (as shown in the inset, scale bar 50 nm). The arrow indicates the wire growth direction.

testing. In figure 3(c), we performed SAD for the broken Ni NW sample (as shown in the inset, corresponding to the right part in figure 3(b)) and it showed that the residual nanowire remained as an fcc structure in the [112] orientation ($R_2/R_1 = \sim 1.3$, $\varphi = \sim 78^\circ$, zone axis (345)). Interestingly, additional diffraction spots were also observed as compared to the original SAD pattern of the same sample before mechanical testing (image not shown), which may indicate that the fracture zone might have undergone some local reorientations in the crystalline structure. Finally, it should be noted that the yield of such experiments inside a TEM is still quite low due to various sample damaging mechanisms associated with nanoindenter tip engagement with the top shuttle of the devices and mechanical translational movement of the TEM sample holder during the initial stage of the mechanical testing. Future improvements are clearly needed to make full use of this novel testing set-up.

4. Conclusions

Here, we have demonstrated that the recently developed micro-mechanical device could be utilized to perform intriguing

quantitative mechanical testing of nanoscale samples inside a TEM assisted by a high precision TEM-nanoindenter holder. With careful consideration and improvement in the design and experimental set-up, metallic nanowires were successfully tested and such *in situ* TEM experiments showed its strength and potential of not only ensuring accurate and valid measurements via real-time video monitoring but also revealing the internal structural evolution while providing precise force–displacement measurements. Therefore, the reported *in situ* TEM set-up could effectively facilitate the construction of the much desired structure–(mechanical) property relationship with quantitative understanding at the nanoscale, with the possibility of testing a wide variety of different low-dimensional nanoscale materials.

Acknowledgments

The authors acknowledge the financial support provided by the Air Force Office of Sponsored Research (AFOSR) YIP award FA9550-09-1-0084, by the Air Force Research Laboratory grant AFRL FA8650-07-2-5061 and by NSF grants ECCS-0702766 and CMMI-0800896. This work was performed,

in part, at the Center for Integrated Nanotechnologies, a US Department of Energy, Office of Basic Energy Sciences user facility at Los Alamos National Laboratory (contract DE-AC52-06NA25396) and Sandia National Laboratories (contract DE-AC04-94AL85000). Sandia National Laboratories is a multi-program laboratory operated by Sandia Corporation, a wholly owned subsidiary of Lockheed Martin Company, for the US Department of Energy's National Nuclear Security Administration under contract DE-AC04-94AL85000.

References

- [1] Huang M H, Mao S, Feick H, Yan H, Wu Y, Kind H, Weber E, Russo R and Yang P 2001 Room-temperature ultraviolet nanowire nanolasers *Science* **292** 1897–9
- [2] Xia Y, Yang P, Sun Y, Wu Y, Mayers B, Gates B, Yin Y, Kim F and Yan H 2003 One-dimensional nanostructures: synthesis, characterization, and applications *Adv. Mater.* **15** 353–89
- [3] Law M, Goldberger M and Yang P 2004 Semiconductor nanotubes and nanowires *Annu. Rev. Mater. Res.* **34** 83–122
- [4] Liu Z and Searson P C 2006 Single nanoporous gold nanowire sensors *J. Phys. Chem. B* **110** 4318–22
- [5] Lu W and Lieber C M 2007 Nanoelectronics from the bottom up *Nature Mater.* **6** 841–50
- [6] Minor A M, Asif S S, Shan Z, Stach E A, Cyrankowski E, Wyrobek T J and Warren O L 2006 A new view of the onset of plasticity during the nanoindentation of aluminium *Nature Mater.* **5** 697–702
- [7] Greer J R and Nix W D 2006 Nanoscale gold pillars strengthened through dislocation starvation *Phys. Rev. B* **73** 245410
- [8] Uchic M D, Dimiduk D M, Florando J N and Nix W D 2004 Sample dimensions influence strength and crystal plasticity *Science* **305** 986–9
- [9] Shan Z W, Mishra R K, Asif S S, Warren O L and Minor A M 2007 Mechanical annealing and source-limited deformation in submicrometre-diameter Ni crystals *Nature Mater.* **7** 115–9
- [10] Buzzi S, Dietiker M, Kunze K, Spolenak R and Löffler J F 2009 Deformation behavior of silver submicrometer-pillars prepared by nanoimprinting *Phil. Mag.* **89** 869–84
- [11] Wu B, Heidelberg H and Boland J J 2005 Mechanical properties of ultrahigh-strength gold nanowires *Nature Mater.* **4** 525–9
- [12] Wang M S, Kaplan-Ashiri I, Wei X L, Rosentsveig R, Wagner H D, Tenne R and Peng L M 2008 *In situ* TEM measurements of the mechanical properties and behavior of WS₂ nanotubes *Nano Res.* **1** 22–31
- [13] Hsin C L, Mai W, Gu Y, Gao Y, Huang C T, Liu Y, Chen L J and Wang Z L 2008 Elastic properties and buckling of silicon nanowires *Adv. Mater.* **20** 3919–23
- [14] Poncharal P, Wang Z L, Ugarte D and Heer W A 1999 Electrostatic deflections and electromechanical resonances of carbon nanotubes *Science* **283** 1513–6
- [15] Cimalla V et al 2008 Nanomechanics of single crystalline tungsten nanowires *J. Nanomater.* **2008** 638947
- [16] Agrait N, Rubio G and Vieira S 1995 Plastic deformation of nanometer-scale gold connective necks *Phys. Rev. Lett.* **74** 3995–8
- [17] Kizuka T 1998 Atomistic visualization of deformation in gold *Phys. Rev. B* **57** 11158–63
- [18] Richter G, Hillerich K, Gianola D S, Monig R, Kraft O and Volkert C A 2009 Ultrahigh strength single crystalline nanowhiskers grown by physical vapor deposition *Nano Lett.* **9** 3048–52
- [19] Li X, Chasiotis I and Kitamura T 2010 *In situ* scanning probe microscopy nanomechanical testing *MRS Bull.* **35** 361–7
- [20] Zhu Y, Moldovan N and Espinosa H D 2005 A microelectromechanical load sensor for *in situ* electron and x-ray microscopy tensile testing of nanostructures *Appl. Phys. Lett.* **86** 013506
- [21] Peng B, Locascio M, Zapol P, Li S, Mielke S L, Schatz G C and Espinosa H D 2008 Measurements of near-ultimate strength for multiwalled carbon nanotubes and irradiation-induced crosslinking improvements *Nature Nanotechnol* **3** 626–31
- [22] Demczyk B G, Wang Y M, Cumings J, Hetman M, Han W, Zettl A and Ritchie R O 2002 Direct mechanical measurement of the tensile strength and elastic modulus of multiwalled carbon nanotubes *Mater. Sci. Eng. A* **334** 173–8
- [23] Eppell S J, Smith B N, Kahn H and Ballarini R 2006 Nano measurements with micro devices: mechanical properties of hydrated collagen fibrils *J. R. Soc. Interface* **3** 117–21
- [24] Haque M A and Saif M T A 2004 Deformation mechanisms in free-standing nanoscale thin films: a quantitative *in situ* transmission electron microscope study *Proc. Natl. Acad. Sci. USA* **101** 6335–40
- [25] Shen Z L, Dodge M R, Kahn H, Ballarini R and Eppell S J 2008 Stress-strain experiments on individual collagen fibrils *Biophys. J.* **95** 3956–63
- [26] Zhu Y and Espinosa H D 2005 An electromechanical material testing system for *in situ* electron microscopy and applications *Proc. Natl. Acad. Sci. USA* **102** 14503–8
- [27] Haque M A, Espinosa H D and Lee H J 2010 MEMS for *in situ* testing-handling, actuation, loading, and displacement measurements *MRS Bull.* **35** 375–81
- [28] Lu Y, Ganesan Y and Lou J 2010 A multi-step method for *in situ* mechanical characterization of 1-D nanostructures using a novel micromechanical device *Exp. Mech.* **50** 47–54
- [29] Ganesan Y, Lu Y, Peng C, Lu H, Ballarini R and Lou J 2010 Development and application of a novel micro-fabricated device for *in situ* tensile testing of 1-D nanomaterials, *J. Microelectromech. Syst.* **19** 675–82
- [30] Ganesan Y, Peng C, Lu Y, Ci L, Srivastava A, Ajayan P M and Lou J 2010 Effects of nitrogen doping on the mechanical properties of carbon nanotubes *ACS Nano* **4** 7637–43
- [31] Zhang L, Petit T, Lu Y, Kratochvil B, Peyer K, Pei R, Lou J and Nelson B 2010 Controlled propulsion and cargo transport of rotating nickel nanowires near a patterned solid surface *ACS Nano* **4** 6228–34
- [32] Salem A K, Searson P C and Leong K W 2003 Multifunctional nanorods for gene delivery *Nature Mater.* **2** 668–71
- [33] Nafari A, Karlen D, Rusu C, Svensson K, Olin H and Enoksson P 2008 MEMS sensor for *in situ* TEM atomic force microscopy *J. Microelectromech. Syst.* **17** 328–33
- [34] Howatson A M, Lund P G and Todd J D 1991 *Engineering Tables and Data* 2nd edn (London: Chapman and Hall) p 41
- [35] Agrawal R, Peng B and Espinosa H D 2009 Experimental-computational investigation of ZnO nanowires strength and fracture *Nano Lett.* **9** 4177–83
- [36] Gall K, Diao J and Dunn M L 2004 The strength of gold nanowires *Nano Lett.* **4** 2431–6
- [37] Zheng H, Cao A, Weinberger C R, Huang J Y, Du K, Wang J, Ma Y, Xia Y and Mao S X 2010 Discrete plasticity in sub-10 nm-sized gold crystals *Nature Commun.* **1** 144